The effect of core–shell particles on the mechanical performance of epoxy resins modified with hyperbranched polymers

Shuiping Li
School of Materials Engineering, Yancheng Institute of Technology, Jiangsu Yancheng, 224051, People's Republic of China; and College of Materials Science and Engineering, Nanjing University of Science and Technology, Jiangsu Nanjing, 210094, People's Republic of China

Qing Lin
School of Materials Engineering, Jinling Institute of Technology, Jiangsu Nanjing, 211169, People's Republic of China

Chong Cui[a)]
College of Materials Science and Engineering, Nanjing University of Science and Technology, Jiangsu Nanjing, 210094, People's Republic of China

(Received 21 September 2015; accepted 8 April 2016)

A novel core–shell particle that consists of epoxide-terminated hyperbranched polymer (HBP) and silica nanoparticles was incorporated into an epoxy/hydroxyl-terminated HBP blend to fabricate a high-performance epoxy thermoset. The effect of the core–shell particle content on the mechanical properties of the epoxy thermosets was investigated in detail. Results from tensile, flexural, and impact tests are provided. The impact fracture surface was studied by field emission-scanning electron microscopy. The incorporation of 2 wt% core–shell particles improved the tensile strength, percent elongation at break, flexural strength, and impact resistance of epoxy/hydroxyl-terminated HBP thermosets. Field emission-scanning electron micrographs showed that core–shell particle addition resulted in large-scale shear deformation and debonding from the epoxy matrix, and improved the epoxy resin toughness.

I. INTRODUCTION

Epoxy resins are one of the most developed high-temperature thermoset materials and they are used extensively as a structural adhesive, functional coating, mechanical and electronic material, molding compound, and advanced composite matrix.[1] These extensive application prospects result from their versatile properties, such as high strength, stiffness and modulus, creep resistance, good thermal stability, electrical properties, adhesive strength, and excellent chemical and corrosion resistance.[2] However, a well-known drawback of epoxy resins is their brittleness, which results from their high crosslinking character. This leads to a poor resistance to crack formation and crack growth, which restricts their application significantly.[3]

Several methods have been proposed to improve the toughness of epoxy resins.[4] Reactive liquid rubbers are well-known as effective fillers to improve toughness.[5] The phase separation of rubber particles after curing results in matrix shear yielding and plastic deformation.[6] However, major defects of this method include decreases in material thermal and elastic properties.[7] Silica nanoparticles have been used to enhance the epoxy resin toughness,[8,9] because these nanoparticles can increase the toughness without sacrificing the thermo-mechanical properties and the glass transition temperature (T_g).[10,11] Bray et al. suggests that the epoxy toughness increases steadily with increasing silica nanoparticle content.[12] Blackman et al. demonstrated that the introduction of silica nanoparticles into an epoxy polymer increased the fracture toughness and cyclic-fatigue behavior.[13] However, the relatively high specific surface area of nanoparticles also increases the resin viscosity significantly, which reduces the ease of processing.[14] An organic/inorganic hybrid route has been considered for the preparation of silica-based hybrid particles. These hybrids can combine advantages of silica particles and organic polymers. Hence, it is tempting to modify silica nanoparticles with rubbers. Pan and He provided a novel approach to prepare core–shell pentablock copolymer/silica hybrids by growing silica on pentablock copolymer precursors.[15] Zeng et al. suggested an approach to fabricate epoxy-functionalized polystyrene/silica core–shell hybrid nanoparticles via emulsion polymerization.[16] The strength and modulus of epoxy thermosets with silica/rubber hybrids were higher than those of the thermoset that was modified only with rubber.[17] Gao et al. proposed that SiO_2 nanoparticles grafted by rubbery

Contributing Editor: Linda S. Schadler
[a)]Address all correspondence to this author.
e-mail: cuichongnust@163.com
DOI: 10.1557/jmr.2016.174

 © Materials Research Society 2016

https://doi.org/10.1557/jmr.2016.174 Published online by Cambridge University Press

block copolymer enhanced the ductility, fracture toughness, and fatigue crack growth resistance of the epoxy matrix substantially.[18] Multiscale hybrid composites were fabricated using carbon nanotubes[19] and graphene was grown on carbon nanotube[20] with an epoxy matrix. Jiang et al. introduced silica nanoparticles that attached to graphene oxide into epoxy to enhance the mechanical properties of the composites.[21] The effects of silica nanoparticle/multiwalled carbon nanotubes,[22] carbon nanotubes/microparticles,[23] and silica sand nanoparticle/glass fiber hybrids on epoxy-based composites have been reported.[24]

Recently, the addition of core–shell particles (CSPs) has proven to be a good solution to solve toughness problems in epoxy resins.[25] Chen and co-workers showed that pre-formed polysiloxane rubber CSPs were well-dispersed into epoxy resins and did not affect the T_g.[26] Naguib et al. showed that the presence of CSPs did not affect the curing process but improved the impact resistance.[27] Meng et al. introduced spherical core–shell nanodomains with average diameters of 29 or 32 nm into epoxy thermosets.[28] Quan and Ivankovic confirmed that the interaction between matrix and particles increased the T_g, ductility, and Poisson's ratio, but reduced the Young's modulus and tensile strength.[29] However, the introduction of traditional CSPs that consist of pure polymers as core and shell parts has resulted in the decrease of other mechanical properties, such as tensile and flexural strength.[25] An important strategy to fabricate CSPs with high mechanical properties is to prepare hybrid core–shell composites composed of functional organic polymers and inorganic nanoparticles.[30] An advantage of this approach is that these hybrid CSPs can combine the versatile characteristics and properties of organic polymers and the excellent physical properties of inorganic nanoparticles. The addition of CSPs, that consist of silica nanoparticles as core and poly(methyl methacrylate) as shell, improved the toughness of epoxy-based composites without any significant deterioration in their thermal properties.[31]

Hyperbranched polymers (HBPs), which have a low viscosity and melting point, unique three-dimensional architecture, and compatibility with other polymers,[32] are used to improve the impact resistance of epoxy resins.[33] An exceptional characteristic of HBPs is their high density of terminal functional groups, which can enhance the compatibility between HBPs and epoxy matrices. Tomuta et al. demonstrated that the introduction of HBPs toughened epoxy.[34] Allauddin et al. observed an improvement in the thermal stability, T_g, storage modulus, tensile strength, and toughness of epoxy/HBP thermosets.[35]

Many investigations have been conducted on the improvement in the mechanical properties of epoxy resins. However, increased attention should be given to their extensive application. In this paper, the goal was to focus on improving the mechanical performance of epoxy resins by using newly designed CSPs and hydroxyl-terminated HBPs (HBPHs). The novelty of this work is the synergistic reinforcement of epoxy resins with CSPs and HBPH. The effect of CSP content on the mechanical properties of epoxy/HBPH thermosets was studied. Results from tensile, flexural, and impact tests are discussed. The impact fracture surface microstructure was observed using field emission-scanning electron microscopy (FESEM).

II. EXPERIMENTAL

A. Materials

Diglycidyl ether of bisphenol A epoxy resin E51 with an epoxide equivalent value of 185–208 g/eq. was obtained from Hangzhou (Wuhuigang Adhesive Co., Ltd., China). Polyamide 650 with an amine value of 220 ± 20 mg KOH/g, which was synthesized by the polymerization of eleostearic acid monomers and diethylenetriamine, was purchased from Wuxi (WuxiResin Factory, China). Silica nanoparticles of an average 50-nm diameter were obtained from Yixing (Xinxing Co., Ltd, China). Aqueous solutions of hydrogen peroxide (H_2O_2, 30 wt%), toluene (98%), γ-aminopropyl triethoxysilane (98%), *N*,*N*-dimethylacetamide (98%, DMA), epichlorohydrin (98%, ECH), succinic anhydride (98%), and diethanolamine (98%) were purchased from Chengdu (Kelong Chemical Reagent Company, China).

B. HBPH synthesis

HBPH synthesis followed the method in former reports.[36–38] Succinic anhydride (1.57 g) was blended with diethanolamine (1.50 g) at 70 °C for 6 h in a 50-mL round-bottomed flask provided with a thermometer, nitrogen inlet, and magnetic stirring. The mixture was heated to 120 °C and kept for 6 h with stirring in nitrogen. The HBPH product was dried at 80 °C for 12 h under vacuum to eliminate the water formed.

C. Preparation of CSPs

Typically, silica nanoparticles (0.5 g) were blended with 5-mL H_2O_2 solution and sonicated for 30 min in a 50-mL three-neck round-bottomed flask, followed by refluxing at 105 °C for 4 h with magnetic stirring. After drying at 80 °C under vacuum overnight, particles were added into 5-mL toluene and sonicated for 30 min. γ-Aminopropyl triethoxysilane (0.25 g) was added and the mixture was heated to 80 °C for 24 h with magnetic stirring under nitrogen. The silanized particles were also dried at 80 °C under vacuum overnight. The modified particles were blended homogeneously with diethanolamine (0.5 g) with magnetic stirring at 300 rpm for 30 min. Succinic anhydride (0.52 g) was added and

https://doi.org/10.1557/jmr.2016.174 Published online by Cambridge University Press

heated to 70 °C for 6 h with magnetic stirring, followed by heating to 120 °C for another 6 h under nitrogen. After cooling to 110 °C, ECH (6.12 g) was added dropwise and stirred for 6 h. The resulting products were re-dissolved in DMA, followed by filtering to eliminate the undissolved materials and drying at 80 °C for 24 h under vacuum. The CSP fabrication route is shown in Scheme 1.

D. Preparation of epoxy thermosets

To prepare the epoxy, a mixture of the appropriate amounts of epoxy resin and HBPH (HBPH/epoxy, 0.16:1 w/w according to our former work[36]) was blended by mechanical stirring at 300 rpm for 30 min. Then CSPs (CSPs/epoxy, 0, 1, 2, 3, 4, 5 wt%) were added into the homogeneous mixture and sonicated at 30 °C for 30 min to improve the CSP dispersion. After that, polyamide 650 (650/epoxy, 1.2:1 w/w, calculated based on the reaction of active hydrogen and epoxide, and preheated to 60 °C to improve the processability) was added and the resulting mixture was homogenized by mechanical stirring at 300 rpm for 10 min. Finally, the mixtures were poured into stainless steel templates and cured at 60 °C for 48 h in an oven.

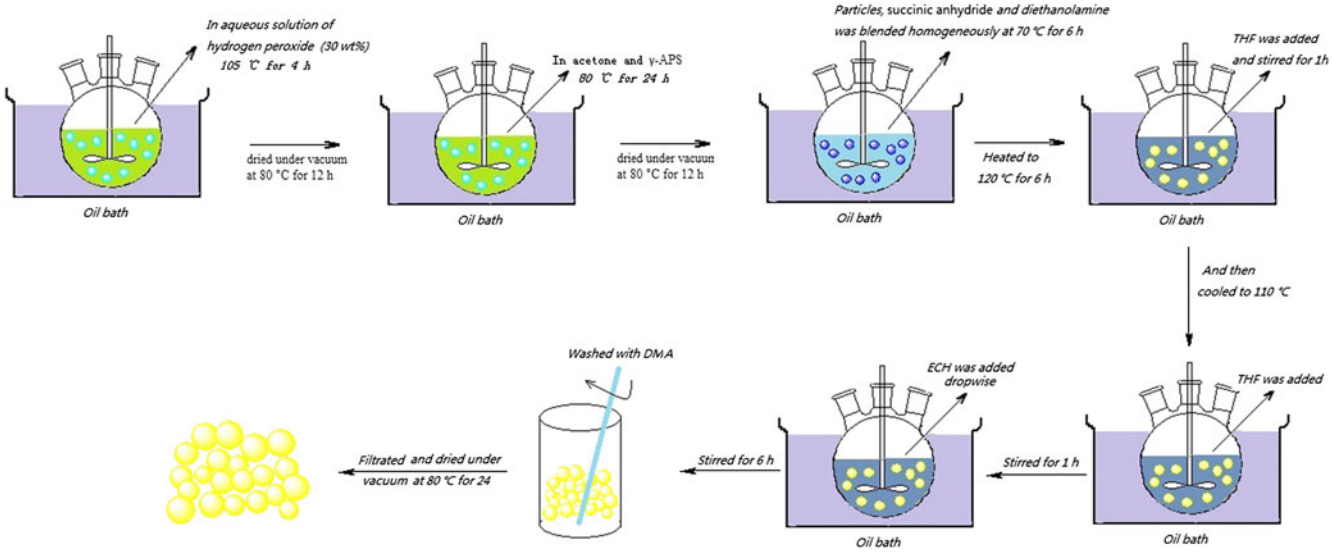
E. Characterization

Infrared spectroscopy spectra were obtained with a Tensor 37 instrument (Germany, Bruker) at a resolution of 2 cm^{-1} and from 400 to 4000 cm^{-1} by attenuated total internal reflectance Fourier transform infrared spectroscopy (ATR-IR). Nuclear magnetic resonance (NMR) analyses were recorded on an AVANCE III 500 NMR spectrometer (Switzerland, Bruker) with deuterated dimethyl sulfoxide (DMSO-d_6) as the solvent at 20 °C. CSP (50 mg) was added into a 5-mL beaker with 1 mL DMSO-d_6 with magnetic stirring at 300 rpm for 2 h. The mixture was centrifuged at 1678 g for 10 min. The supernatant liquid was used for ^{1}H NMR spectra tests. A DTG 60 simultaneous measuring instrument (Japan, SHIMADZU) from 30 to 800 °C at 20 °C/min was used to evaluate the thermogravity of the nanoparticles before and after surface modification. High-resolution transmission electron micrographs were obtained using a Tecnai 20 electron microscope (USA, FEI). The particles were dispersed in ethanol and sonicated for 10 min. Then the suspension was transferred to a copper grid with a carbon film using a dropper and dried at room temperature. Differential scanning calorimetry of epoxy thermosets was performed with a 200 F3 differential scanning calorimeter from −30 to 300 °C at 20 °C/min under nitrogen (Germany, NETZSCH). Tensile tests were performed on a dog-bone-shaped sample according to GB/T 2567-2008 standard with an AG-X plus test machine (Japan, SHIMADZU). The flexural strength was characterized by an UTM4000 electromechanical universal testing machine (China, SANS) according to GB/T 2567-2008 standard at room temperature with dimensions of 80 × 15 × 4 mm and a loading rate of 2 mm/min. Unnotched Izod tests were performed on a ZBC-50 impact tester (China, SANS) using a GB/T 2567-2008 standard with 4-mm thickness and 10-mm width. All results were an average of five specimens. After impact testing, the fracture surface was observed with a SU8000 FESEM (Japan, Hitachi), and the fracture surface of the thermosets was sputter-coated with gold before observation.

III. RESULTS AND DISCUSSION

A. CSP characterization

The ATR-IR spectra of the pristine silica, silanized silica, and CSPs are shows in Fig. 1. The broad peak at



SCHEME 1. The fabrication route of CSPs.

https://doi.org/10.1557/jmr.2016.174 Published online by Cambridge University Press

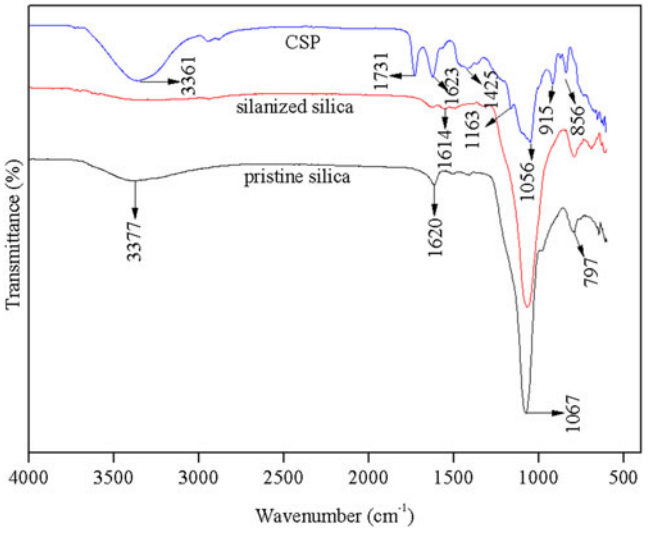


FIG. 1. The ATR-IR spectra of pristine silica, silanized silica and CSPs.

3377 cm^{-1} in the ATR-IR spectrum of pristine silica can be assigned to the asymmetric –OH stretching. The weak band at 1620 cm^{-1} is attributed to the H–OH bending. The sharp absorptions at 1067 and 797 cm^{-1} are assigned to –OH and Si–O stretching, respectively. In contrast with the ATR-IR spectrum of pristine silica, two different parts are observed in the ATR-IR spectrum of silanized silica particles. The broad absorptions at 3377 and 1620 cm^{-1} disappeared. A new peak appeared at 1614 cm^{-1}, which can be ascribed to N–H stretching. This peak is the characteristic absorption band of siloxane linkages. In the ATR-IR spectrum of CSPs, the broad absorption at 3361 cm^{-1} can be attributed to intermolecular hydrogen bonding stretching. Absorptions at 1163 and 1731 cm^{-1} are assigned to asymmetric C–O and –C=O stretching, respectively. The weak peaks at 1623 and 1425 cm^{-1} are attributed to N–H stretching and C–N bending, respectively. The appearance of peaks at 1056, 915, and 856 cm^{-1} (epoxy group) confirms the reaction between HBPH and ECH and hence the formation of epoxy bonds. All absorptions indicate that terminal epoxide groups exist in the CSP shell layer.

NMR spectroscopy is a useful and substantive technique for polymer characterization, and provides a deeper insight into the polymer chemical structure. The representative ^{1}H NMR spectrum of CSP also provides more detailed evidence to prove the successful grafting of epoxide-terminated HBP (HBPE) on the silanized silica particles surface, as shown in Fig. 2. Peaks existed at 2.49 ppm (–CH_2CHCH_2O–, protons a), 2.93 ppm (–CH_2CHCH_2O–, protons b), 3.52 ppm (–CH_2CHCH_2O–, protons c), 3.63 ppm (N–CH_2–CH_2–O–, protons d), 3.48 ppm (N–CH_2–CH_2–O–, protons e), 2.62 ppm (O=CH_2–CH_2=O, protons f), 3.59 ppm (O=CH_2–CH_2=O, protons g), 3.89 ppm (N–CH_2–CH_2–O, protons h) and 2.77 ppm (N–CH_2–CH_2–O, protons i). The peaks at 2.49, 2.93, and 3.52 ppm are characteristic of an epoxide ring, which indicates the successful fabrication of CSPs. The peaks at 2.49, 2.93, and 3.52 ppm are attributed to protons of the terminal units. The peaks at 3.63 and 3.48 ppm are ascribed to those of the dendritic units, whereas, those at 2.62, 2.77, 3.59, and 3.89 ppm can be attributed to protons of the linear units.

The thermo-gravimetric analysis (TGA) curves of hydroxylated silica, silanized silica, and CSPs measured under nitrogen are shown in Fig. 3. The temperatures for 5 and 10 wt% mass loss ($T_{5\%}$ and $T_{10\%}$) from the CSPs are 65.8 and 118.1 °C, respectively. The mass losses of the hydroxylated silica, silanized silica, and CSPs are 18.7, 30.3, and 43.3% at 800 °C, respectively, and increase as hydroxylated silica particles < silanized silica particles < CSPs. This may provide evidence of the successful grafting of γ-aminopropyl triethoxysilane and HBPE on the silica nanoparticle surface. CSPs exhibit a high mass loss (24.1%) at low temperature (from the onset degradation temperature to 300 °C), which is consistent with reports in the literature.[39,40] The mass loss of CSPs (13.0%) is higher than that of boron nitride functionalized by HBP (BN-HBP) (5.13%)[41] and HBP grafted barium titanate (BT-HBP) (4.91%).[42] This is attributed to the difference in hydroxyl group density (–OH) that is available for chemical bonding of nanoparticles. The surface of the hydroxylated silica particles has a large amount of hydroxyl groups, which can contact the amino groups of the silane-coupling agent. Thus, the percentage grafting of HBPE on the silanized silica particle surface is higher than that in other works.

The transmission electron microscopy (TEM) image of the CSPs, as shown in Fig. 4, shows the nanoparticle size, shape, and dispersion. CSPs agglomerate slightly owing to the strong polarity of their terminal epoxide groups, high specific surface area, and surface energy. The CSP sizes range from 60 to 80 nm.

B. Glass transition temperature

The T_gs of the epoxy thermosets are listed in Table I. The neat epoxy displays a T_g at 143 °C. Those of epoxy/HBPH thermosets with 0, 1, 2, 3, 4, and 5 wt% CSPs are 141, 140, 141, 144, 145, and 145 °C, respectively. The increase in T_g may be ascribed to a high polarity of the epoxide groups grafted on the CSP surface, which can modify the epoxy thermoset network and inhibit the segmental motion of the epoxy.[43]

C. Mechanical performance

The incorporation of HBPs can improve the impact toughness of the epoxy resins but may sacrifice other mechanical properties, such as the tensile and flexural strength, because of the introduction of flexible chains in

https://doi.org/10.1557/jmr.2016.174 Published online by Cambridge University Press

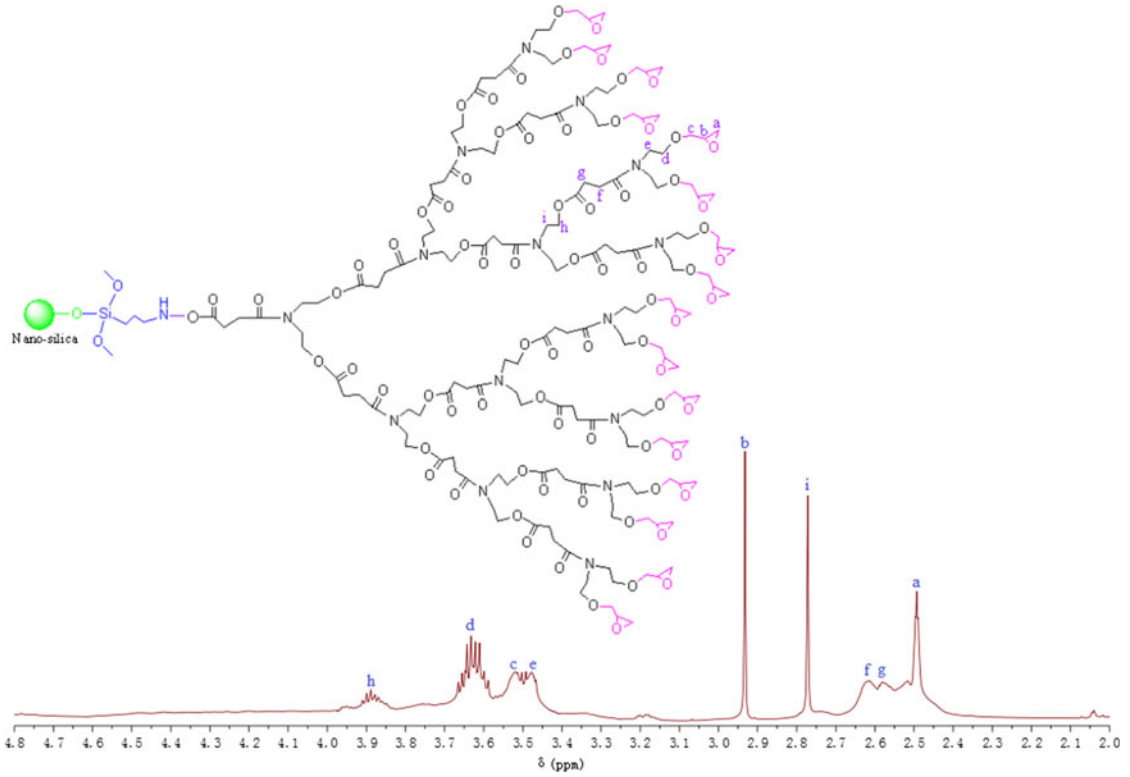


FIG. 2. ^{1}H NMR spectrum of CSPs.

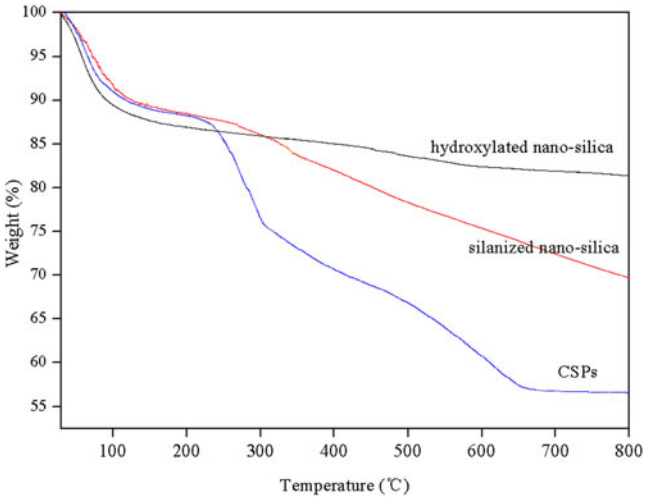


FIG. 3. TGA curves of hydroxylated nanosilica, silanized nanosilica and CSPs measured under N_2.

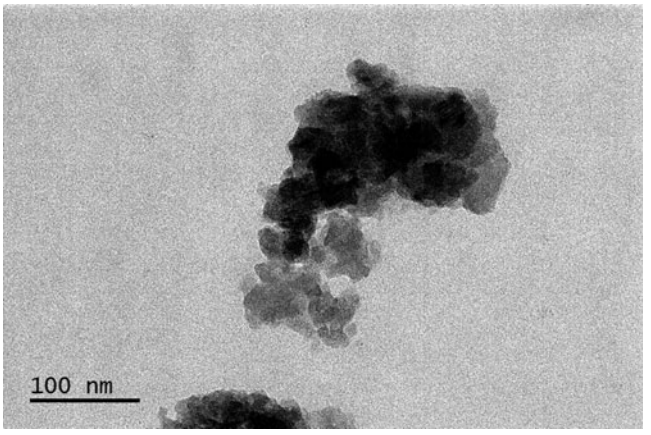


FIG. 4. TEM micrograph of CSP.

TABLE I. The glass transition temperatures (T_gs) of the epoxy composites[a].

CSP content (wt%)	T_g (°C)	CSP content (wt%)	T_g (°C)
Neat epoxy	143	3	144
0	141	4	145
1	140	5	145
2	141	...	...

[a]Neat epoxy means the epoxy thermosets without neither HBPH nor CSP.

their frameworks.[44] Our previous report demonstrated that an incorporation of 16 wt% HBPH could improve the impact strength by ~32.8% but decrease the flexural strength of the epoxy resins.[36] To improve the epoxy thermoset strength, some rigid phases should be incorporated into epoxy resins, such as nanoparticles, carbon tubes, or CSPs, which were mentioned above. In this work, a new type of CSP that consists of HBPE and silica nanoparticles was chosen as a good solution. Figure 5 shows the variation in tensile strength and percent elongation at break as a function of CSP content. As shown in Fig. 5(a), the tensile strength of the epoxy/HBPH

https://doi.org/10.1557/jmr.2016.174 Published online by Cambridge University Press

thermoset with 0 wt% CSP is lower than that of the neat epoxy. The tensile strength increases with increasing amount of CSP in the epoxy/HBPH thermosets. The maximum tensile strength improves by 46% with an addition of 2 wt% CSP compared with that at 0 wt%. It is difficult to summarize and predict the tensile strength of epoxy resin because this mechanical property depends mainly on the strength of the weakest part of the test specimens, instead of the average strength.[29] The addition of HBPH increases the percent elongation at break compared with the neat epoxy [Fig. 5(b)], which may be attributed to the low crosslink density and the special HBPH spherical shape. Lv et al. suggested that the spherical HBPH molecule had a loose architecture and made the epoxy matrix softer than neat epoxy.[44] The decrease can be attributed to CSP aggregation.

Figure 6 shows the flexural strength of epoxy/HBPH thermosets with different CSP contents. The flexural strength increases from 46.6 MPa for the unmodified epoxy/HBPH thermoset to 81.4 MPa for the formulation with 2 wt% CSPs. Thereafter, the trend alters and the flexural strength decreases to 51.4 MPa for the thermoset with 5 wt% CSPs. The maximum value increases by ~29.8% and 74.7%, compared with the neat epoxy and unmodified epoxy/HBPH thermoset, respectively. Figure 7 shows the impact strength of epoxy/HBPH thermosets as a function of CSP content. Similarly, the impact strength increases with CSP content, which shows a reduction in increasing trend. All modified epoxy/HBPH thermosets show a higher impact resistance than that of the neat epoxy. By comparison with the neat epoxy and other epoxy/HBPH thermosets, the formulation with 2 wt% CSPs shows the highest impact strength of 15.709 kJ/m^2. These results indicate that the impact resistance of epoxy/HBPH thermosets can be improved by the addition of a small amount of CSPs. However, the CSPs may be easily agglomerated especially when the CSP concentration exceeds the percolation threshold.[45] Aggregation can induce stress concentration and result in crack initiation and a reduction in interfacial interaction between the nanoparticles and the polymer matrix.[46] In conclusion, epoxy thermosets with excellent impact resistance are obtained.

Wang et al. proposed a yield function to quantify the effects of tensile stress on the plastic yielding behavior of rubber-modified epoxies and found good agreement with experimental results.[47] Chen et al. demonstrated that the predictions of the Halpin–Tsai and the Lewis–Nielsen models showed good agreement with the experimental data.[26] Quan and Ivankovic also suggested that the addition of core–shell rubber nanoparticles reduced the tensile strength of epoxy reins according to the experiment and model prediction.[29] Different from rubber particles filled epoxy, CSP incorporation can improve

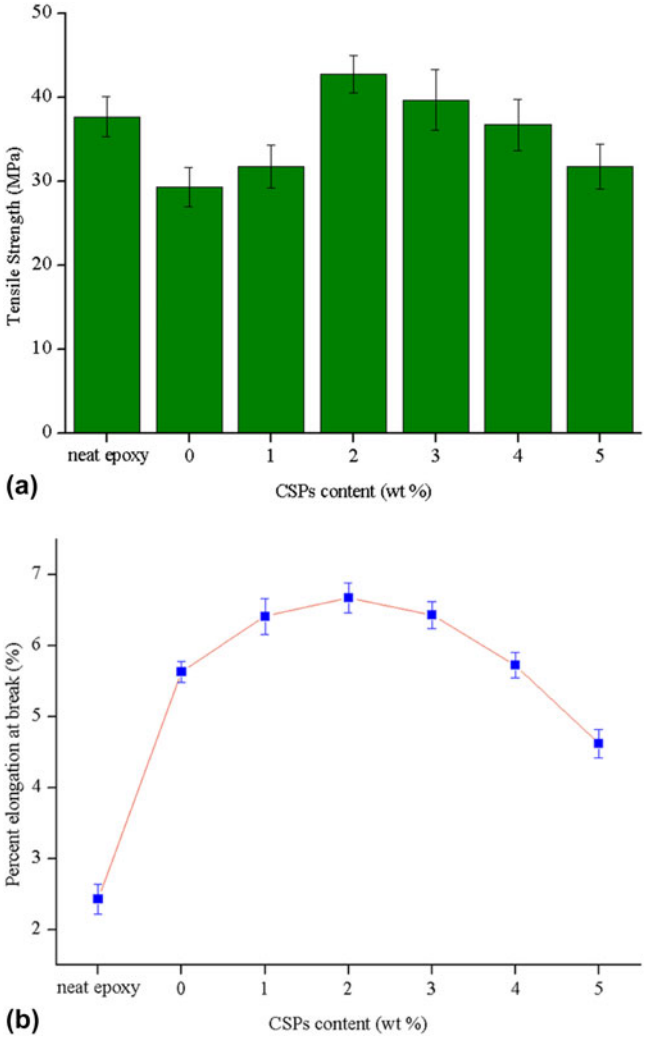


FIG. 5. (a) Tensile strength (b) and percent elongation at break of epoxy/HBPH thermosets as function of CSPs content.

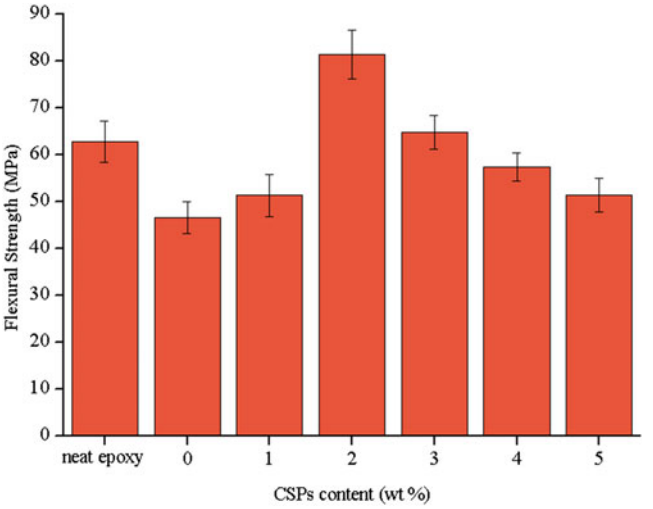


FIG. 6. Flexural strength of epoxy/HBPH thermosets as function of CSPs content.

https://doi.org/10.1557/jmr.2016.174 Published online by Cambridge University Press

the strength and impact toughness because of the synergistic effect of the rigidity of silica nanoparticles and the excellent compatibility between HBPE and the epoxy matrix. The reason for this improvement can be explained by the following four aspects: firstly, the enhancement in mechanical properties of epoxy/HBPH thermosets modified with CSPs can be attributed to the interaction between epoxide groups attached to the silanized silica particle surfaces and hydroxyl groups in epoxy resins.[33] Secondly, the formed domains, which are attributed to the incorporation of CSPs, can withstand a greater mechanical loading from the matrix when the matrix is under stress.[28,48] This means that when the applied loading exceeds the elastic deformation stress, the CSPs have a stress transfer effect and enhances the strength and plasticity of the epoxy matrix.[49] Thirdly, CSPs can produce more microcrack surface area, which leads to an increase in the epoxy thermoset toughness.[48] Finally, the enhanced impact toughness may originate from the crack tip pinning/bridging effect of the CSP chemically bonded to the epoxy matrix, which is similar to other reported epoxy that is toughened by rigid nanofillers.[50] However, the mechanical properties of epoxy/HBPH thermosets are expected to undergo decay if the CSP content exceeds 2 wt%. Although, the graft of HBPE on the silanized silica particle surface can improve the compatibility between CSPs and epoxy matrix; the dispersion of CSPs in epoxy resins worsens with CSP content and results in a defect in the epoxy matrix.[33]

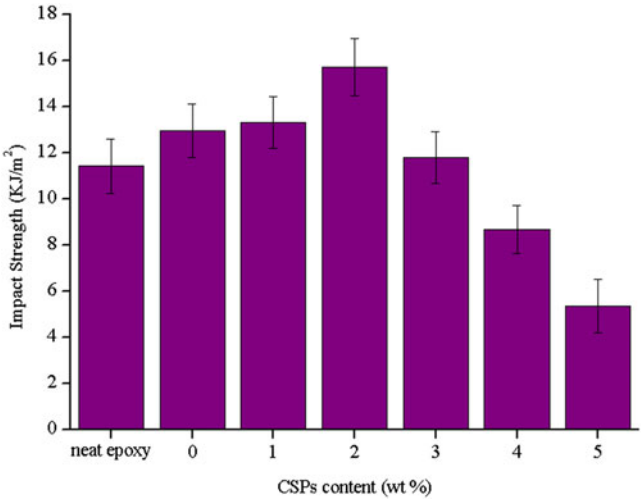


FIG. 7. Impact strength of epoxy/HBPH thermosets as function of CSPs content.

D. Morphological analysis

The impact behavior of epoxy thermosets can be explained in terms of the morphology observed by FESEM. The fracture surface morphologies of epoxy thermosets are shown in Fig. 8. The fracture surface of the neat epoxy indicates a brittle fracture with no uninterrupted crack propagation path and leads to poor resistance to crack initiation and propagation [Fig. 8(a)]. The fracture surface morphology of the unmodified

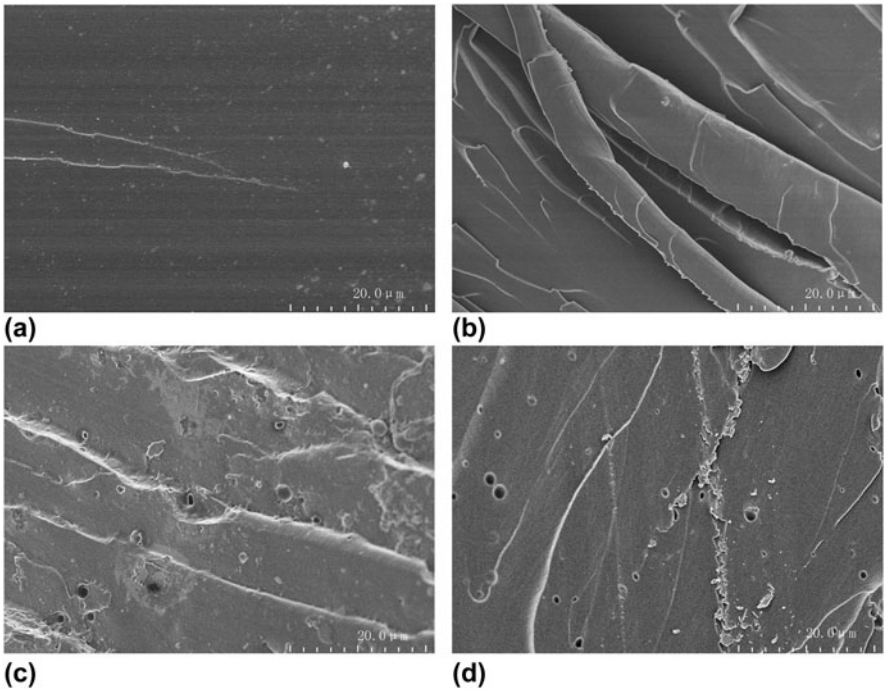


FIG. 8. FESEM images of (a) neat epoxy thermoset, (b) epoxy/HBPH thermoset, (c) epoxy/HBPH thermoset with 2 wt%, and (d) 5 wt% CSPs.

https://doi.org/10.1557/jmr.2016.174 Published online by Cambridge University Press

epoxy/HBPH thermoset [Fig. 8(b)] presents a homogeneous appearance without any phase separation. This phenomenon can account for the good compatibility between the epoxy matrix and the HBPH. This morphology also exhibits a rough and coarse surface that contains a large number of propagated cracks, crack deflection and shear deformation. This may result from the high density of hydroxyl groups in the HBPH architecture. The epoxy/HBPH thermoset morphology with 2 wt% CSPs shows several large shear deformations and crack propagation [Fig. 8(c)]. CSPs can induce stress concentrations, which lead to extensive shear deformation.[44] When cracks initiate, the shear deformation can absorb fracture energy[51] and interrupt crack propagation. The CSPs disperse uniformly in this thermoset, which indicates the good compatibility between CSPs and epoxy matrix in the HBPH.[27] Several exposed CSPs debond from the epoxy matrix. The morphological characterization highlights several cavities, which are ascribed to the debonding of embedded CSPs from the epoxy matrix. CSP debonding absorbs impact energy and improves the epoxy resin impact resistance. Thus, the use of an appropriate amount of CSPs can improve the impact resistance of epoxy/HBPH thermosets. However, the fracture surface morphology of the thermoset with 5 wt% CSPs shows large crack propagation from CSP aggregation [Fig. 8(d)]. The impact energy has been absorbed and is focused on these aggregates, which results in deterioration in impact resistance.

IV. CONCLUSIONS

A new CSP has been prepared by grafting HBPE on the surface of silanized silica nanoparticles. The CSP was used as a toughening modifier of epoxy resin modified with HBPH. The effect of the CSP content on the mechanical properties of epoxy thermosets was investigated. The toughening mechanisms were identified and discussed.

The results show that the T_gs of epoxy/HBPH thermosets increase with CSP content. The tensile strength, percent elongation at break, flexural strength, and impact strength of epoxy/HBPH thermosets were also improved. For instance, the tensile strength, percent elongation at break, flexural strength, and impact strength of the epoxy/HBPH thermoset modified with 2 wt% CSPs were 42.77 MPa, 6.67%, 81.41 MPa, and 15.709 kJ/m^2, respectively. These values represent improvements of 45.97, 18.47, 74.71, and 21.18%, respectively, compared with unmodified epoxy/HBPH thermoset.

Based on our results, the use of CSPs may be a feasible approach to increase the mechanical properties of epoxy resin modified with HBPH.

ACKNOWLEDGMENTS

The authors gratefully acknowledge supports from the National Natural Science Foundation of China (51402251, 51578289, 51572234 and 51502259), the National Science and Technology Major Project of the Ministry of Science and Technology of China (2012ZX04010032), the joint research fund between Collaborative Innovation Center for Ecological Building Materials and Environmental Protection Equipments and Key Laboratory for Advanced Technology in Environmental Protection of Jiangsu Province (CP201506 and GX2015107), the project funded by the Flagship Major Development of Jiangsu Higher Education Institutions (PPZY2015A025), and the Natural science fund of Jiangsu Province (BK20130428).

REFERENCES

1. A.A. Azeez, K.Y. Rhee, S.J. Park, and D. Hui: Epoxy clay nanocomposites—Processing, properties and applications: A review. *Composites, Part B* **45**(1), 308–320 (2013).
2. S. Zaioncz, A.A. Silva, A.S. Sirqueira, and B.G. Soares: Toughening of epoxy resin by methyl methacrylate/2-ethylhexyl acrylate copolymers: The effect of copolymer composition. *Macromol. Mater. Eng.* **292**(12), 1263–1270 (2007).
3. M. DeCarli, K. Kozielski, W. Tian, and R. Varley: Toughening of a carbon fibre reinforced epoxy anhydride composite using an epoxy terminated hyperbranched modifier. *Compos. Sci. Technol.* **65**(14), 2156–2166 (2005).
4. N. Domun, H. Hadavinia, T. Zhang, T. Sainsbury, G.H. Liaghat, and S. Vahid: Improving the fracture toughness and the strength of epoxy using nanomaterials—A review of the current status. *Nanoscale* **7**(23), 10294–10329 (2015).
5. S. Kar and A.K. Banthia: Synthesis and evaluation of liquid amine-terminated polybutadiene rubber and its role in epoxy toughening. *J. Appl. Polym. Sci.* **96**(6), 2446–2453 (2005).
6. L-C. Tang, X. Wang, Y-J. Wan, L-B. Wu, J-X. Jiang, and G-Q. Lai: Mechanical properties and fracture behaviors of epoxy composites with multi-scale rubber particles. *Mater. Chem. Phys.* **141**(1), 333–342 (2013).
7. P. Hazot, C. Pichot, and A. Maazouz: Synthesis of hairy acrylic core–shell particles as toughening agents for epoxy networks. *Macromol. Chem. Phys.* **201**(6), 632–641 (2000).
8. S. Sprenger, M.H. Kothmann, and V. Altstaedt: Carbon fiber-reinforced composites using an epoxy resin matrix modified with reactive liquid rubber and silica nanoparticles. *Compos. Sci. Technol.* **105**, 86–95 (2014).
9. A. Dorigato, A. Pegoretti, and M. Quaresimin: Thermo-mechanical characterization of epoxy/clay nanocomposites as matrices for carbon/nanoclay/epoxy laminates. *Mater. Sci. Eng., A* **528**(19–20), 6324–6333 (2011).
10. M. Crespo, M. González, and J. Pozuelo: Magnetic silica:epoxy composites with a nano- and micro-scale control. *Mater. Chem. Phys.* **144**(3), 335–342 (2014).
11. A.J. Kinloch, K. Masania, A.C. Taylor, S. Sprenger, and D. Egan: The fracture of glass-fibre-reinforced epoxy composites using nanoparticle-modified matrices. *J. Mater. Sci.* **43**(3), 1151–1154 (2008).
12. D.J. Bray, P. Dittanet, F.J. Guild, A.J. Kinloch, K. Masania, R.A. Pearson, and A.C. Taylor: The modelling of the toughening of epoxy polymers via silica nanoparticles: The effects of volume fraction and particle size. *Polymer* **54**(26), 7022–7032 (2013).

https://doi.org/10.1557/jmr.2016.174 Published online by Cambridge University Press

13. B.R.K. Blackman, A.J. Kinloch, J.S. Lee, A.C. Taylor, R. Agarwal, G. Schueneman, and S. Sprenger: The fracture and fatigue behaviour of nano-modified epoxy polymers. *J. Mater. Sci.* **42**(16), 7049–7051 (2007).
14. S.O. Ilyin, T.V. Brantseva, I.Y. Gorbunova, S.V. Antonov, Y.M. Korolev, and M.L. Kerber: Epoxy reinforcement with silicate particles: Rheological and adhesive properties—Part I: Characterization of composites with natural and organically modified montmorillonites. *Int. J. Adhes. Adhes.* **61**, 127–136 (2015).
15. A. Pan and L. He: Formation and properties of core–shell pentablock copolymer/silica hybrids. *Mater. Chem. Phys.* **147**(1–2), 5–10 (2014).
16. Z. Zeng, J. Yu, and Z-X. Guo: Preparation of epoxy-functionalized polystyrene/silica core–shell composite nanoparticles. *J. Polym. Sci., Part A: Polym. Chem.* **42**(9), 2253–2262 (2004).
17. A.J. Kinloch, R.D. Mohammed, A.C. Taylor, C. Eger, S. Sprenger, and D. Egan: The effect of silica nano particles and rubber particles on the toughness of multiphase thermosetting epoxy polymers. *J. Mater. Sci.* **40**(18), 5083–5086 (2005).
18. J. Gao, J. Li, S. Zhao, B.C. Benicewicz, H. Hillborg, and L.S. Schadler: Effect of graft density and molecular weight on mechanical properties of rubbery block copolymer grafted SiO_2 nanoparticle toughened epoxy. *Polymer* **54**(15), 3961–3973 (2013).
19. S.P. Sharma and S.C. Lakkad: Impact behavior and fractographic study of carbon nanotubes grafted carbon fiber-reinforced epoxy matrix multi-scale hybrid composites. *Composites, Part A* **69**, 124–131 (2015).
20. H. Im and J. Kim: Thermal conductivity of a graphene oxide-carbon nanotube hybrid/epoxy composite. *Carbon* **50**(15), 5429–5440 (2012).
21. T. Jiang, T. Kuila, N.H. Kim, B-C. Ku, and J.H. Lee: Enhanced mechanical properties of silanized silica nanoparticle attached graphene oxide/epoxy composites. *Compos. Sci. Technol.* **79**, 115–125 (2013).
22. X. Jia, B. Liu, L. Huang, D. Hui, and X. Yang: Numerical analysis of synergistic reinforcing effect of silica nanoparticle–MWCNT hybrid on epoxy-based composites. *Composites, Part B* **54**, 133–137 (2013).
23. W. Li, D. He, and J. Bai: The influence of nano/micro hybrid structure on the mechanical and self-sensing properties of carbon nanotube-microparticle reinforced epoxy matrix composite. *Composites, Part A* **54**, 28–36 (2013).
24. T. Ahmad, R. Ahmad, M. Kamran, B. Wahjoedi, I. Shakoor, F. Hussain, F. Riaz, Z. Jamil, S. Isaac, and Q. Ashraf: Effect of Thal silica sand nanoparticles and glass fiber reinforcements on epoxy-based hybrid composite. *Iran. Polym. J.* **24**(1), 21–27 (2015).
25. D. Quan and A. Ivankovic: Effect of core–shell rubber (CSR) nano-particles on mechanical properties and fracture toughness of an epoxy polymer. *Polymer* **66**, 16–28 (2015).
26. J. Chen, A.J. Kinloch, S. Sprenger, and A.C. Taylor: The mechanical properties and toughening mechanisms of an epoxy polymer modified with polysiloxane-based core–shell particles. *Polymer* **54**(16), 4276–4289 (2013).
27. M. Naguib, S. Grassini, and M. Sangermano: Core/shell PBA/PMMA–PGMA nanoparticles to enhance the impact resistance of UV-cured epoxy systems. *Macromol. Mater. Eng.* **298**(1), 106–112 (2013).
28. Y. Meng, X-H. Zhang, B-Y. Du, B-X. Zhou, X. Zhou, and G-R. Qi: Thermosets with core–shell nanodomain by incorporation of core crosslinked star polymer into epoxy resin. *Polymer* **52**(2), 391–399 (2011).
29. D. Quan and A. Ivankovic: Effect of core–shell rubber (CSR) nano-particles on mechanical properties and fracture toughness of an epoxy polymer. *Polymer* **66**, 16–28 (2015).
30. Z. Su, B. Yu, X. Jiang, and J. Yin: Hybrid core–shell microspheres from coassembly of anthracene-containing POSS (POSS-AN) and anthracene-ended hyperbranched poly(ether amine) (hPEA-AN) and their responsive polymeric hollow microspheres. *Macromolecules* **46**(9), 3519–3528 (2013).
31. P. Yang, L.Y. Zhu, X. Xia, H.T. Wang, Q.G. Du, and W. Zhong: Toughening of epoxy resin with poly(methyl methacrylate) grafted silica core–shell particles. *e-Polym.* **11**, 710–721 (2011).
32. S. Thakur and N. Karak: Ultratough, ductile, castor oil-based, hyperbranched, polyurethane nanocomposite using functionalized reduced graphene oxide. *ACS Sustainable Chem. Eng.* **2**(5), 1195–1202 (2014).
33. L. Pan, S. Lu, X. Xiao, Z. He, C. Zeng, J. Gao, and J. Yu: Enhanced mechanical and thermal properties of epoxy with hyperbranched polyester grafted perylene diimide. *RSC Adv.* **5**(5), 3177–3186 (2015).
34. A. Tomuta, F. Ferrando, À. Serra, and X. Ramis: New aromatic–aliphatic hyperbranched polyesters with vinylic end groups of different length as modifiers of epoxy/anhydride thermosets. *React. Funct. Polym.* **72**(9), 556–563 (2012).
35. S. Allauddin, M.K. Akhil Chandran, K.K. Jena, R. Narayan, and K.V.S.N. Raju: Synthesis and characterization of APTMS/melamine cured hyperbranched polyester-epoxy hybrid coatings. *Prog. Org. Coat.* **76**(10), 1402–1412 (2013).
36. S. Li, C. Cui, H. Hou, Q. Wu, and S. Zhang: The effect of hyperbranched polyester and zirconium slag nanoparticles on the impact resistance of epoxy resin thermosets. *Composites, Part B* **79**, 342–350 (2015).
37. S. Li, C. Cui, and H. Hou: Synthesis of core–shell particles based on hyperbranced polyester and zirconium slag nanoparticles and its influence on the impact resistance of epoxy resin thermosets. *Polym. Compos.* (2015). doi: 10.1002/pc.23602.
38. S. Li, Q. Lin, H. Zhu, H. Hou, Y. Li, Q. Wu, and C. Cui: Improved mechanical properties of epoxy-based composites with hyperbranched polymer grafting glass-fiber. *Polym. Adv. Technol.* (2016). doi: 10.1002/pat.3746.
39. X. Huang, M.S. Heo, J-W. Yoo, J-S. Choi, and I. Kim: Hyperbranched aliphatic polyether esters by ring-opening polymerization of epoxidized 2-hydroxyethyl methacrylate. *J. Polym. Sci., Part A: Polym. Chem.* **52**(12), 1643–1651 (2014).
40. Y. Zhang, D. Zhang, C. Qin, and J. Xu: Physical and mechanical properties of dental nanocomposites composed of aliphatic epoxy resin and epoxidized aromatic hyperbranched polymers. *Polym. Compos.* **30**(2), 176–181 (2009).
41. J. Yu, X. Huang, C. Wu, X. Wu, G. Wang, and P. Jiang: Interfacial modification of boron nitride nanoplatelets for epoxy composites with improved thermal properties. *Polymer* **53**(2), 471–480 (2012).
42. L. Xie, X. Huang, Y. Huang, K. Yang, and P. Jiang: Core–shell structured hyperbranched aromatic polyamide/$BaTiO_3$ hybrid filler for poly(vinylidene fluoride-trifluoroethylene-chlorofluoroethylene) nanocomposites with the dielectric constant comparable to that of percolative composites. *ACS Appl. Mater. Interfaces* **5**(5), 1747–1756 (2013).
43. R. Qian, J. Yu, L. Xie, Y. Li, and P. Jiang: Efficient thermal properties enhancement to hyperbranched aromatic polyamide grafted aluminum nitride in epoxy composites. *Polym. Adv. Technol.* **24**(3), 348–356 (2013).
44. S. Lv, Y. Yuan, and W. Shi: Strengthening and toughening effects of layered double hydroxide and hyperbranched polymer on epoxy resin. *Prog. Org. Coat.* **65**(4), 425–430 (2009).
45. R.P. Wang, T. Schuman, R.R. Vuppalapati, and K. Chandrashekhara: Fabrication of bio-based epoxy–clay nanocomposites. *Green Chem.* **16**(4), 1871–1882 (2014).

https://doi.org/10.1557/jmr.2016.174 Published online by Cambridge University Press

46. B. Qi, Q.X. Zhang, M. Bannister, and Y.W. Mai: Investigation of the mechanical properties of DGEBA-based epoxy resin with nanoclay additives. *Compos. Struct.* **75**(1–4), 514–519 (2006).
47. X. Wang, K. Xiao, L. Ye, Y-W. Mai, C.H. Wang, and L.R.F. Rose: Modelling mechanical properties of core–shell rubber-modified epoxies. *Acta Mater.* **48**(2), 579–586 (2000).
48. V.K. Srivastava: Modeling and mechanical performance of carbon nanotube/epoxy resin composites. *Mater. Des.* **39**, 432–436 (2012).
49. J. Zhang and D. Jiang: Interconnected multi-walled carbon nanotubes reinforced polymer–matrix composites. *Compos. Sci. Technol.* **71**(4), 466–470 (2011).
50. W. Thitsartarn, X. Fan, Y. Sun, J.C.C. Yeo, D. Yuan, and C. He: Simultaneous enhancement of strength and toughness of epoxy using POSS–rubber core–shell nanoparticles. *Compos. Sci. Technol.* **118**, 63–71 (2015).
51. G.G. Buonocore, L. Schiavo, I. Attianese, and A. Borriello: Hyperbranched polymers as modifiers of epoxy adhesives. *Composites, Part B* **53**, 187–192 (2013).

https://doi.org/10.1557/jmr.2016.174 Published online by Cambridge University Press